Repository of the Max Delbrück Center for Molecular Medicine (MDC) in the Helmholtz Association

http://edoc.mdc-berlin.de/13245

Common gating of both CLC subunits underlies voltage-dependent activation of the 2Cl-/1H+-exchanger ClC-7/Ostm1

Ludwig, C.F., Ullrich, F., Leisle, L., Stauber, T., Jentsch, T.J.

Common Gating of Both CLC Transporter Subunits Underlies Voltage-dependent Activation of the 2Cl⁻/1H⁺ Exchanger ClC-7/Ostm1*

Carmen F. Ludwig[‡§]**, Florian Ullrich**[‡§]**, Lilia Leisle**[‡§1]**, Tobias Stauber**[‡§]**, and Thomas J. Jentsch**[‡§¶2]

From the [‡]*Leibniz-Institut für Molekulare Pharmakologie (FMP) and* [§]*Max-Delbrück-Centrum für Molekulare Medizin (MDC), D-13125 Berlin and the* [¶]*NeuroCure Cluster of Excellence, Charité Universitätsmedizin Berlin, 10117 Berlin, Germany*

Background: ClC-7 is a homodimeric lysosomal chloride transporter important for lysosomal function and bone degradation.

Results: Altered gating kinetics of one subunit affect the kinetics of the other subunit.

Conclusion: Gating of ClC-7 involves both CLC subunits and requires noncovalent binding of cytoplasmic domains.

Significance: Osteopetrosis and lysosomal storage disease are associated with accelerating mutations in the ClC-7 C terminus and the contacting intramembrane part.

CLC anion transporters form dimers that function either as Cl⁻ channels or as electrogenic Cl⁻/H⁺ exchangers. CLC channels display two different types of "gates," "protopore" gates that open and close the two pores of a CLC dimer independently of each other and common gates that act on both pores simultaneously. ClC-7/Ostm1 is a lysosomal 2Cl⁻/1H⁺ exchanger that is slowly activated by depolarization. This gating process is drastically accelerated by many *CLCN7* mutations underlying human osteopetrosis. Making use of some of these mutants, we now investigate whether slow voltage activation of plasma membrane-targeted ClC-7/Ostm1 involves protopore or common gates. Voltage activation of wild-type ClC-7 subunits was accelerated by co-expressing an excess of ClC-7 subunits carrying an accelerating mutation together with a point mutation rendering these subunits transport-deficient. Conversely, voltage activation of a fast ClC-7 mutant could be slowed by co-expressing an excess of a transport-deficient mutant. These effects did not depend on whether the accelerating mutation localized to the transmembrane part or to cytoplasmic cystathionine-β-synthase (CBS) domains of ClC-7. Combining accelerating mutations in the same subunit did not speed up gating further. No currents were observed when ClC-7 was truncated after the last intramembrane helix. Currents and slow gating were restored when the C terminus was co-expressed by itself or fused to the C terminus of the β-subunit Ostm1. We conclude that common gating underlies the slow voltage activation of ClC-7. It depends on the CBS domain-containing C terminus that does not require covalent binding to the membrane domain of ClC-7.

The CLC gene family, first identified by the cloning of the voltage-dependent Cl⁻ channel ClC-0 from *Torpedo* electric organ (1), not only encodes Cl⁻ channels, but also encodes anion/proton exchangers (2–5). Both CLC Cl⁻ channels and Cl⁻/H⁺ exchangers function as homodimers with one ion translocation pathway per pore, as shown by mutational structure/function analysis (6–8) and x-ray crystallography of prokaryotic and algal CLC proteins (9, 10). Four of the nine mammalian CLC proteins associate with distinct small accessory subunits that display one or two transmembrane domains (11–13). For instance, the lysosomal 2Cl⁻/1H⁺ exchanger ClC-7 requires binding to the type-I transmembrane protein Ostm1 for protein stability and ion transport activity (12, 14).

The ion transport activity of both CLC Cl⁻ channels and Cl⁻/H⁺ exchangers can strongly depend on the transmembrane voltage. Voltage-dependent gating has been most thoroughly studied with the fish ClC-0 Cl⁻ channel. Macroscopic currents and single-channel analysis provided clear evidence for two distinct gating processes in ClC-0: a fast, depolarization-activated protopore gate acting independently on each of the two pores of the dimer and a slow, hyperpolarization-activated common gate closing both pores simultaneously (15–17). Likewise, mammalian ClC-1 and ClC-2 display protopore and common gating, but their time constants and voltage dependences, as well as the low single-channel conductances of these channels, render the identification and separation of these gating modes more difficult (18–22). The crystal structure of bacterial EcClC-1, together with mutagenesis, showed that a certain "gating" glutamate, whose side chain protrudes into the ion translocation pathway, plays a pivotal role in protopore gating of CLC channels (23) and in Cl⁻/H⁺ coupling of CLC exchangers (5), findings that were amply confirmed in other studies with prokaryotic and eukaryotic CLCs. The structural basis of common gating is much less understood, but the gating glutamate may also play a role in closing the permeation pathway after a common rearrangement of both subunits (24, 25). Early mutagenesis studies have implicated the cystathionine-β-synthase (CBS)[3] domain-containing C terminus of ClC-0 in its

[1] Present address: University of Iowa, Iowa City, 52242 IA.

[2] To whom correspondence should be addressed: FMP/MDC, Robert-Rössle-Strasse 10, D-13125 Berlin, Germany. Fax: 49-30-9406-2960; E-mail: Jentsch@fmp-berlin.de.

[3] The abbreviations used are: CBS, cystathionine-β-synthase; CT, C terminus; td, transport-deficient.

slow common gating (26), and more recent studies revealed C-terminal movements during common gating of ClC-0 and ClC-1 (27, 28). However, mutations in other regions also affect common gating. For instance, the C212S mutation that totally abolishes slow gating of ClC-0 (29) involves a residue close to the extracellular face of the transmembrane segment.

The mammalian CLC Cl^-/H^+ exchangers (ClC-3 through ClC-7), which are predominantly expressed in the endosomal-lysosomal system (30), are strongly voltage-dependent and mediate measurable ion transport only at positive cytoplasmic potentials (14, 31–34). As currents mediated by ClC-3 through ClC-6 respond very quickly to changes in membrane potential, it is difficult to attribute their voltage dependence either to a gating process that turns the ion exchange on and off or to an intrinsic voltage dependence of the exchange process. Using a plasma membrane-targeted mutant of the lysosomal ClC-7 anion/proton exchanger (35), we recently found that ClC-7/Ostm1 currents respond very slowly to voltage changes (14). These slow current relaxations enabled us to show that the strong outward rectification of ClC-7/Ostm1 is owed to a voltage-dependent gating of the $2Cl^-/1H^+$ exchange process that intrinsically shows an almost linear voltage dependence (14). Mutations either in ClC-7 or in its β-subunit Ostm1 lead to osteopetrosis, lysosomal storage disease, and neurodegeneration in mice and humans (12, 36–39). Interestingly, several human *CLCN7* mutations identified in osteopetrosis drastically accelerate the gating of ClC-7/Ostm1, suggesting that slow gating may be needed for its physiological function (14). Several of these mutations affect residues in the cytoplasmic CBS domains or in nearby loops of the membrane part of ClC-7. In the present work, we use some of these accelerating mutations, in combination with other mutants and biophysical analysis, to show that the gating of ClC-7/Ostm1 involves the common gate. By extension, these findings probably also apply to the other mammalian $2Cl^-/1H^+$ exchangers in which gating cannot be studied easily.

EXPERIMENTAL PROCEDURES

Expression Constructs—All constructs for heterologous expression in *Xenopus laevis* oocytes were cloned into the pTLN expression vector (40) as described (14). Point mutations, insertions, and deletions were introduced into human ClC-7 by recombinant PCR. All constructs were confirmed by sequencing the complete open reading frame. To delete the ClC-7 C terminus, a stop codon was introduced at position 624 (ClC-7$_{C624X}$, or ClC-7$_{\Delta CT}$ for short). C-terminal residues 617–805 were either expressed as a *bona fide* soluble protein (ClC-7$_{CT}$) or fused to the last amino acid of Ostm1 (Ostm1-ClC-7$_{CT}$).

Voltage Clamp of X. laevis Oocytes—*X. laevis* oocytes were injected with cRNA transcribed as described (14) using the mMESSAGE mMACHINE kit (Ambion) according to the following scheme: WT (wild-type hClC-7) + Ostm1, 23 ng + 23 ng; fast gating mutant + Ostm1, 23 ng + 23 ng; WT + fast gating mutant/E314A + Ostm1, 7 ng + 28 ng + 12 ng; fast gating mutant + E314A + Ostm1, 7 ng + 28 ng + 12 ng; ClC-7$_{\Delta CT}$ + Ostm1, 15 ng + 15 ng; ClC-7$_{\Delta CT}$ + ClC-7$_{CT}$ + Ostm1, 15 ng + 15 ng + 15 ng; ClC-7$_{\Delta CT}$ + Ostm1-ClC-7$_{CT}$, 23 ng + 23 ng; insertion/deletion mutants + Ostm1, 23 ng + 23

ng. Oocytes were kept for 3 days at 17 °C before currents were measured using a two-electrode voltage clamp employing TurboTEC amplifiers (npi electronic GmbH, Tamm, Germany) and pClamp 10 Software (Molecular Devices). Oocytes were superfused with ND96 saline (96 mM NaCl, 2 mM potassium gluconate, 1.8 mM calcium gluconate, 1 mM magnesium gluconate, 5 mM HEPES, pH 7.5). In some experiments, NaCl was replaced with equimolar amounts of $NaNO_3$. Currents were evoked by clamping the cells for 2 s to voltages between −80 mV and 80 mV in 20-mV steps followed by a repolarizing step to −80 mV for 500 ms. Leak and capacitive currents were not compensated for, but in the figures, capacitive transients were removed for clarity. Time constants of activation and deactivation were obtained from monoexponential fits to the current trace from 25 to 275 ms after the voltage step to 80 mV or to −80 mV following a 2-s pulse to 80 mV, respectively. To determine relative nitrate conductance, the same oocyte was measured both in standard ND96 and in ND96 in which Cl^- was replaced by NO_3^-. Current amplitudes at 80 mV were normalized to the ones in standard ND96.

RESULTS

As common gating is associated with a coordinate conformational change of both subunits of functional CLC dimers, mutations altering common gating may affect the gating of a wild-type (WT) subunit when present in just one subunit of a WT/mutant heteromer. Indeed, *CLCN1* mutations identified in patients with dominant myotonia that shift the voltage of half-maximal activation ($V_{1/2}$) of homodimeric ClC-1 also shifted the voltage dependence of WT subunits in WT/mutant heteromers (41) by changing common gating (18). In a more extreme case, the slow activation by hyperpolarization of ClC-2 was abolished in ClC-1/ClC-2 heterodimeric channels (40). We therefore argued that human *CLCN7* mutations that lead to faster gating in ClC-7 homodimers (14) should accelerate gating of WT subunits in WT/mutant heterodimers if the activation process involves a common gate. However, changed gating kinetics of different subunits are difficult to disentangle upon 1:1 co-expression of WT and fast mutant subunits as we have to deal with a 1:2:1 mixture of WT/WT, WT/mutant, and mutant/mutant subunits. One may try to solve this problem by forcing the formation of heterodimers by constructing concatemers. Although this approach was successfully applied previously in mixing CLC subunits of different unitary conductances (6, 8, 42), gating kinetics may easily be changed by linking the C terminus of one subunit to the amino terminus of the second one. Indeed, a human ClC-7 frameshift mutant (G796fs) (43) that replaced the last 10 C-terminal residues by 129 foreign ones accelerated ClC-7 gating (14).

We therefore opted to combine in a single subunit a fast mutation with another mutation that abolishes ion transport through the same subunit (see scheme in Fig. 1*A*). Co-expression of this virtually fast, but transport-deficient ("td") mutant at molar excess with WT subunits should result in currents that are dominated by WT subunits present in ClC-7/ClC-7$_{fast,td}$ heteromers. We used the E314A mutation, which will be further referred to as td, to abolish ClC-7/Ostm1 transport activity (14). This mutation neutralizes a "proton glutamate" at the
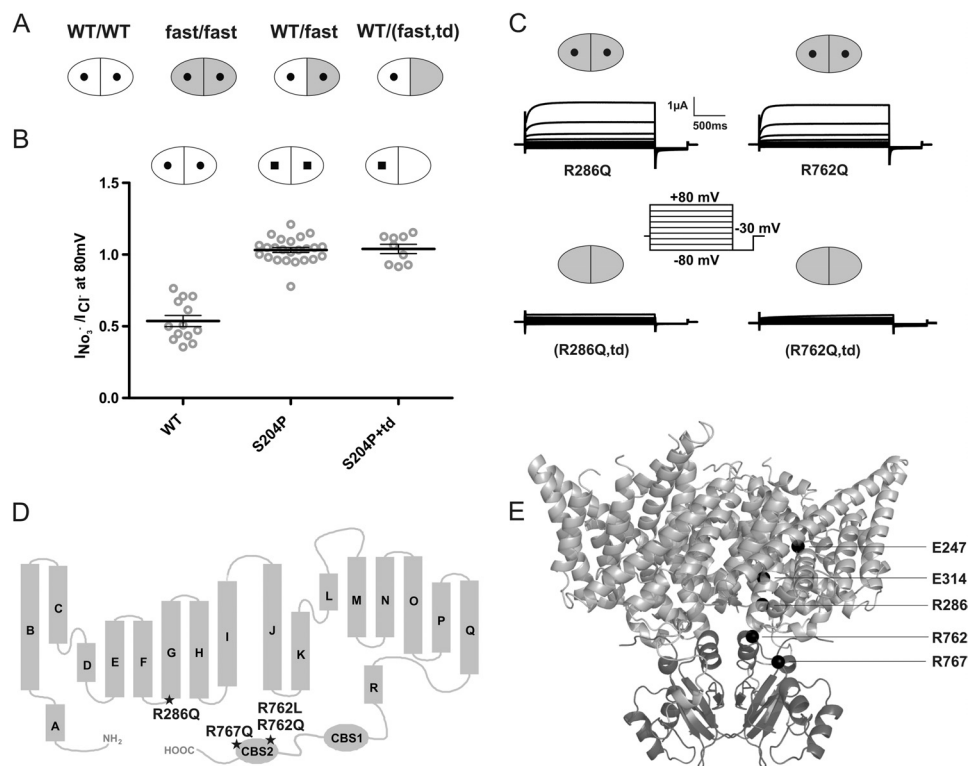
FIGURE 1. **Experimental design and controls.** *A*, schematic presentation of CLC transporter dimers. Each monomer contains an ion permeation pathway. WT subunits are shown in *white*, subunits with an accelerating point mutation are in *gray*, and subunits carrying a transport-abolishing point mutation (td; E314A in ClC-7) are symbolized by a lack of the central "hole." From left, WT/WT, fast/fast, WT/fast, and WT/(fast,td) dimers. *B*, subunits carrying the transport-deficient td mutation do not contribute to currents in WT/td heteromers as probed by differences in nitrate selectivity of WT (round hole) and S204P (square hole) ClC-7 subunits, as indicated by nitrate selectivity of currents that is indistinguishable between S204P/S204P and S204P/td dimers. *Thick lines* in data point clouds indicate arithmetic mean, and *thin lines* indicate ± S.E. *C*, representative voltage clamp traces. The td mutation abolishes currents not only when inserted into WT subunits, but also when inserted into subunits containing the R286Q (*lower left trace*) or R762Q (*lower right trace*) mutations. *D*, topology model of ClC-7 showing the localization of the fast mutations ClC-7$_{R286Q}$, ClC-7$_{R762Q}$, ClC-7$_{R762L}$, and ClC-7$_{R767Q}$. All these mutations underlie human osteopetrosis. *E*, mutations mapped into the crystal structure of algal CmClC. The transmembrane domain is shown in *light gray*, and the CBS domains are in *dark gray*. Positions of the gating (Glu-247 in ClC-7, Glu-210 in CmClC) and proton (Glu-314 in ClC-7, Thr-269 in CmClC) glutamates and of residues Arg-286, Arg-762, and Arg-767 (in ClC-7, corresponding to Leu-241, Val-680, and Ser-685, respectively, in CmClC) are shown as *black spheres*, for clarity only in one of the two subunits.

cytoplasmic face of the transmembrane part of ClC-7 that is thought to be required for the transport of cytoplasmic protons to the Cl$^-$/H$^+$ exchange site at the gating glutamate (44). Mammalian Cl$^-$/H$^+$ exchangers carrying such proton glutamate mutations do not measurably transport Cl$^-$ either (14, 34, 42), probably because Cl$^-$ lacks its exchange partner. This mechanism suggests that the block of ion transport is confined to subunits carrying the td mutation. Although not indicated in the following text, all ClC-7 subunits additionally carried the L23A,L24A and L68A,L69A mutations in N-terminal AP- and GGA-binding sites, respectively, which lead to partial plasma membrane localization of ClC-7 (14, 35). Furthermore, all constructs were co-expressed with the essential β-subunit Ostm1 (12, 14).

We first performed several control measurements to validate our experimental strategy. To confirm that currents of ClC-7/ClC-7$_{td}$ heteromers were only carried by subunits not containing the td mutation, we exploited the effect of the pore mutation S204P that selectively increases nitrate conductance (14, 45, 46). Coexpression of ClC-7$_{S204P}$ with a molar excess of ClC-7$_{td}$ gave rise to currents whose nitrate selectivity was indistinguishable from that of ClC-7$_{S204P}$ homomers (Fig. 1*B*). Hence the td mutation abolishes currents only in the subunit in which it has been inserted, and this effect does not require that the

adjacent subunit of the dimer also carries this mutation. In other control experiments, we ascertained that the td mutation abolished ClC-7 transport activity also when present together with the accelerating mutations R762Q or R286Q in the same subunit (Fig. 1*C*).

For our analysis, we chose three previously characterized (14) fast mutants of ClC-7: R762Q (36) and R767Q (47), mutations in the second CBS domain found in patients with recessive infantile osteopetrosis, and R286Q, which changes a residue in the intracellular loop between intramembrane helices F and G and that has been found in dominant osteopetrosis (47) (for localization of these mutations, see Fig. 1, *D* and *E*). We co-injected oocytes with ClC-7 and ClC-7$_{fast,td}$ cRNAs at a 1:4 ratio (Fig. 2). ClC-7 currents were elicited by 2-s voltage steps to 80 mV. Activation and deactivation kinetics were determined by fitting single exponential equations to currents at the beginning and at the end of the depolarizing voltage step, respectively. Although present in a transport-deficient ClC-7$_{td}$ subunit, all three fast mutations (R286Q, R762Q, and R767Q) markedly accelerated the activation kinetics of ClC-7 currents in *trans* through the attached WT subunit in ClC-7/ClC-7$_{td,fast}$ heteromers. This acceleration did not reach the same levels as observed with homomeric ClC-7$_{fast}$/ClC-7$_{fast}$ transporters (Fig. 2, *A–D*). However, this apparent difference in kinetics is at least

partially owed to currents from WT ClC-7/ClC-7 homodimers, which are estimated to contribute about 20% with our 1:4 ClC-7:ClC-7$_{td,fast}$ co-injection scheme. In the reverse experiment, we asked whether ClC-7$_{fast}$ currents could be slowed down in *trans* by 1:4 co-expression with ClC-7$_{td}$ mutants. This was

indeed the case, and gating kinetics were similar between ClC-7/ClC-7$_{fast,td}$ and ClC-7$_{fast}$/ClC-7$_{td}$ expression schemes for all three accelerating mutants (Fig. 2, *A–D*). Likewise, deactivation kinetics of ClC-7 were accelerated in *trans* by ClC-7$_{td,fast}$ mutants (Fig. 2, *E–G*). In control experiments, ClC-7$_{td}$ did not
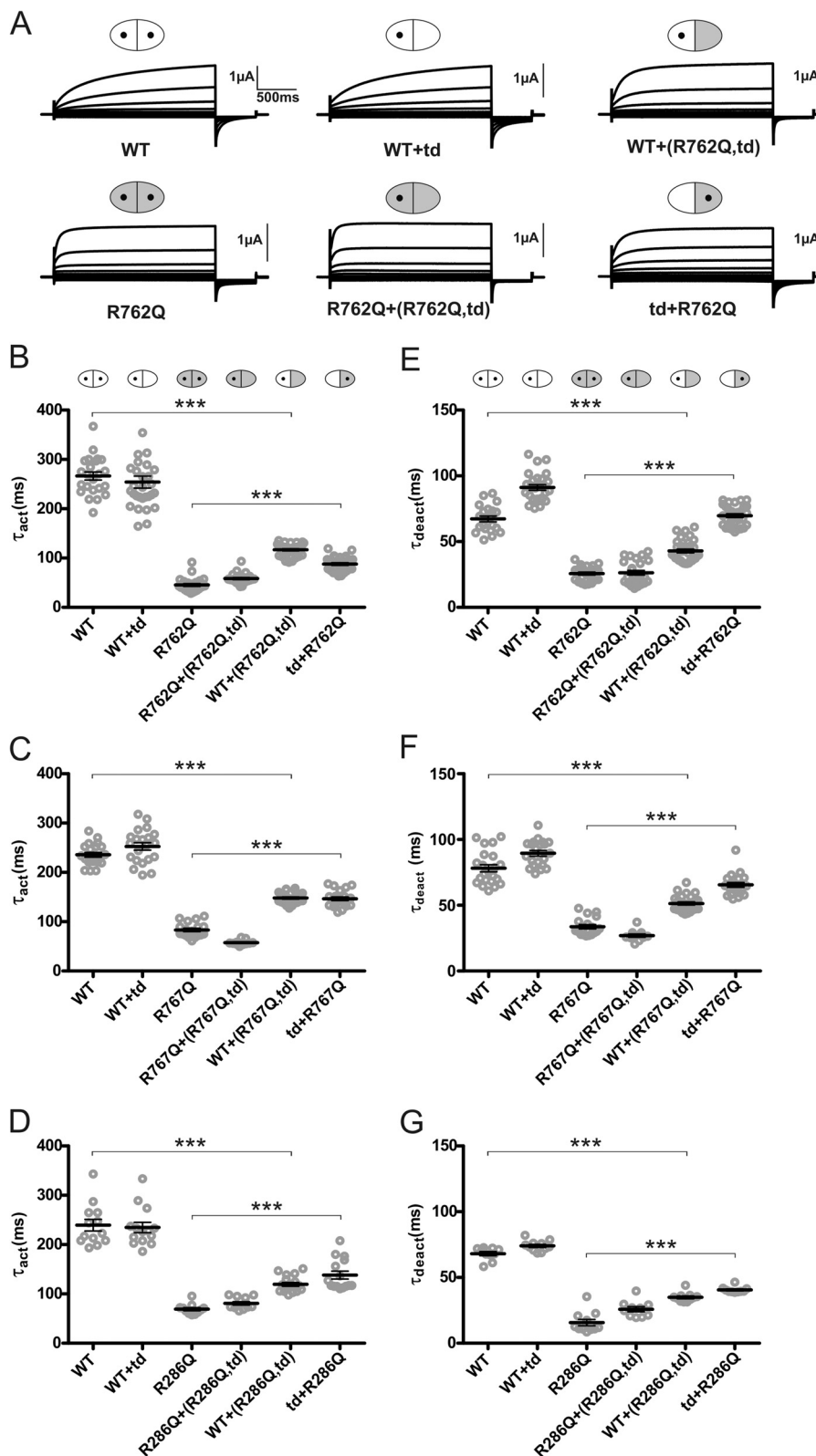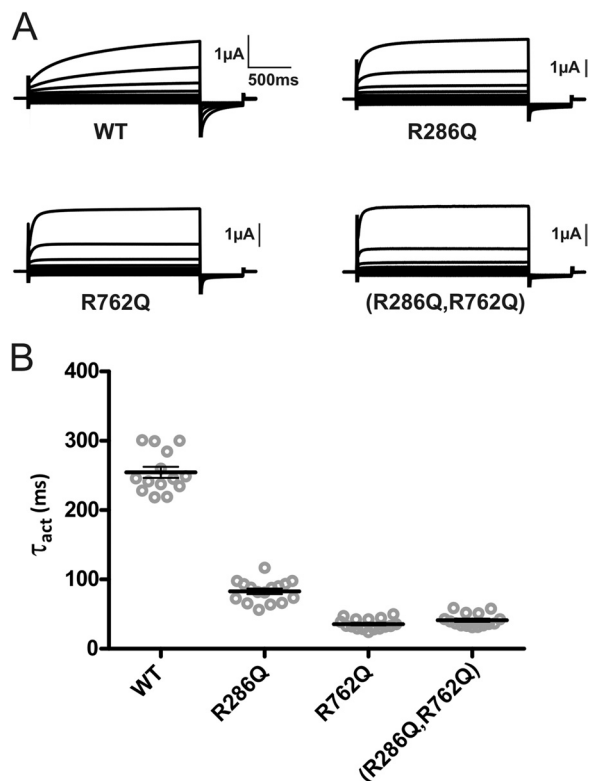
FIGURE 3. **Insertion of two fast mutations into the same subunit does not accelerate gating further.** *A*, original recordings of homodimeric ClC-7 transporters containing the fast mutations R286Q (in the transmembrane domain), R762Q (in CBS2), and R286Q,R762Q double mutants in comparison with wild-type ClC-7. The voltage clamp protocol is as in Fig. 1. *B*, individual and averaged activation time constants (τ_{act}) obtained from those experiments. *Thick lines* indicate arithmetic mean, and *thin lines* indicate ± S.E. The β-subunit Ostm1 was always co-expressed.

affect gating kinetics of co-injected ClC-7, and ClC-7$_{fast}$/ClC-7$_{td,fast}$ displayed gating kinetics similar to ClC-7$_{fast}$ (Fig. 2).

We next asked whether we could further accelerate ClC-7 gating by inserting two fast mutations into the same subunit. We generated the ClC-7 R286Q,R762Q, R286Q,R767Q, and R762Q,R767Q double mutants, out of which only ClC-7$_{R286Q,R762Q}$ gave rise to robust currents (Fig. 3*A*). Time constants of activation of ClC-7$_{R286Q,R762Q}$ and ClC-7$_{R762Q}$ did not differ from each other, showing that the effects of these mutations were not additive (Fig. 3*B*).

Most mutations accelerating the gating of ClC-7 localize to the interface between the cytosolic C terminus and transmembrane domains, where they are thought to disturb gating-relevant interactions (14). On the other hand, the CBS domain-containing C terminus of ClC-7 is covalently attached to intramembrane helix R, which directly coordinates a Cl$^-$ ion in

the CLC pore through the side chain of a tyrosine close to its N terminus (9). It is tempting to speculate that the ClC-7 C terminus influences gating by changing the position of the R-helix. We therefore asked whether the length of the R-CBS1-linker might influence ClC-7 gating. Both deletion and insertion of several amino acids after threonine 621 (Fig. 4*A*) indeed accelerated gating, whereas deleting 6 amino acids abolished ClC-7/Ostm1 transport function (Fig. 4, *B* and C).

These results seemed to support the hypothesis that CBS domains modulate gating by "pulling" on the R-helix. We were curious to know what would happen if we entirely eliminated this possibility by disrupting the peptide bond between helix R and CBS1, using a "split transporter" approach akin to the "split channel" approach as used first with the ClC-1 Cl$^-$ channel (48). Expression of a ClC-7 mutant truncated shortly after the R-helix and thus lacking both CBS domains (ClC-7$_{\Delta CT}$) did not yield currents (Fig. 5, *A* and *B*).

Surprisingly, currents of ClC-7$_{\Delta CT}$ could be rescued by co-expressing the cytoplasmic C terminus (ClC-7$_{CT}$) from a separate cRNA (Fig. 5, *A* and *B*). Resulting currents reached amplitudes similar to WT ClC-7, but their activation kinetics were slightly faster (Fig. 5, *B* and *C*). Instead of expressing the C terminus only as a soluble protein, we also fused it to the obligate ClC-7 β-subunit Ostm1 directly after its last residue to anchor it to the plasma membrane in close vicinity to the ClC-7 backbone. Co-expressing this fusion protein (Ostm1-ClC-7$_{CT}$) with ClC-7$_{\Delta CT}$ (without additional WT Ostm1) yielded currents that were indistinguishable from WT ClC-7/Ostm1 in their kinetics (Fig. 5*C*) and often reached similar amplitudes. We also inserted the fast R762L mutation into CBS2 of the isolated C terminus ClC-7$_{CT}$ and into the Ostm1-ClC-7$_{CT}$ fusion protein. Although the combination of ClC-7$_{\Delta CT}$ + ClC-7$_{CT(R762L)}$ failed to yield currents (data not shown), split channels in which the mutant C terminus was attached to Ostm1 (ClC-7$_{\Delta CT}$ + Ostm1-ClC-7$_{CT(R762L)}$) produced robust currents that displayed activation time constants indistinguishable from the fast mutant ClC-7$_{R762L}$ + Ostm1 (Fig. 5*C*). We conclude that the role of the ClC-7 C terminus in ClC-7 gating does not depend on a covalent linkage to the last intramembrane helix R.

In view of these results, we re-examined the effects of linker deletions (Fig. 4) and expressed split transporters in which the polypeptide chain following helix R was truncated at different positions (Fig. 5*D*). These experiments revealed that gating kinetics became significantly faster when ClC-7 was truncated at position 621 or earlier. Hence the results of our linker shortening might be owed to specific effects of deleting particular

FIGURE 2. **Gating kinetics of ion flux through a ClC-7 monomer are influenced by the adjacent subunit of the dimer.** *A*, effect of the fast R762Q mutation that affects a residue in the second CBS domain. Original voltage clamp traces from oocytes injected with RNA encoding WT ClC-7, ClC-7$_{R762Q}$, a 1:4 ratio of WT and ClC-7$_{R762Q,E314A}$ RNA, and a 1:4 co-injection of the fast ClC-7$_{R762Q}$ mutant with the E314A (td) mutant that renders the subunit transport-deficient are shown. The voltage clamp protocol is as in Fig. 1. Symbols *above* diagrams are as follows: WT subunits are shown in *white*, subunits with an accelerating point mutation are in *gray*, and subunits carrying a transport-abolishing point mutation (td; E314A in ClC-7) are symbolized by a lack of the central "hole." *B*, individual and averaged activation time constants (τ_{act}) obtained from experiments as shown above. Note that transport-deficient fast subunit accelerates gating in dimers with a WT subunit and that the transport-deficient WT subunit slows gating in dimers with a fast subunit, resulting in indistinguishable gating kinetics. *C* and *D*, similar experiments obtained with R767Q, another accelerating mutant in CBS2 (*D*), and with the fast R286Q mutation at the intracellular side of helix G of the membrane part of ClC-7 (*D*). *E*, individual and averaged deactivation time constants (τ_{deact}) of the investigated fast mutant ClC-7$_{R762Q}$. *F* and *G*, similar experiment for ClC-7$_{R767Q}$ (*F*) and ClC-7$_{R286Q}$ (*G*). Oocytes in *E–G* were the same as used in *B–D*. In all experiments, mRNA for the β-subunit Ostm1 was co-injected. *Thick lines* indicate arithmetic mean and *thin lines* indicate ± S.E. *** indicates a *p* value < 0.001 calculated by Student's *t* test between WT and WT+(fast,td), and between fast and td+fast.
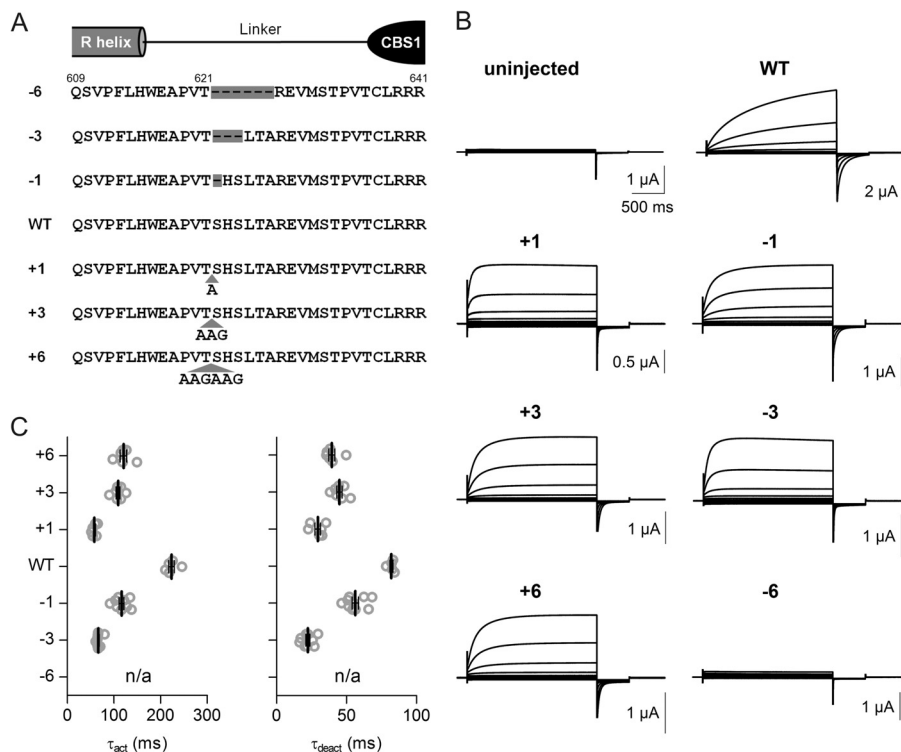
FIGURE 4. **ClC-7/Ostm1 activation kinetics depend on the length of the linker between the transmembrane domain and CBS1.** *A*, diagram showing the sequence of the linker between the last intramembrane helix R and CBS1. Deletion and insertion constructs are shown. *B*, typical two-electrode voltage clamp traces obtained with these constructs upon co-expression with Ostm1. *C*, evaluation of corresponding activation (τ_{act}) and deactivation (τ_{deact}) time constants. The voltage clamp protocol is as in Fig. 1. *Thick lines* indicate arithmetic mean, and *thin lines* indicate $\pm$ S.E.
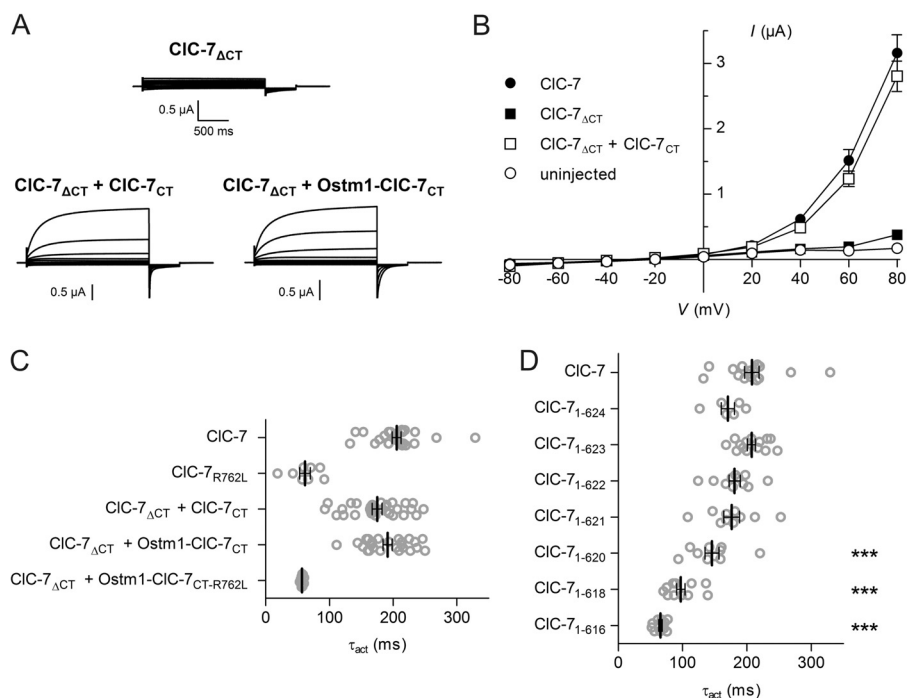
FIGURE 5. **The ClC-7 C terminus is crucial for ClC-7 function and can be supplied as a separate polypeptide chain.** *A*, typical recordings of oocytes expressing ClC-7$_{\Delta CT}$ in which ClC-7 is truncated shortly after the last membrane helix and of oocytes co-expressing this mutant with either the C terminus (ClC-7$_{CT}$) or a chimeric protein (Ostm1-ClC-7$_{CT}$) in which the C terminus is fused to the β-subunit Ostm1. WT Ostm1 was co-expressed in the first two cases. The voltage clamp protocol is as in Fig. 1. *B*, mean near steady-state current-voltage relationships (evaluated at 2 s after voltage steps) obtained from truncated constructs compared with controls. *C*, activation time constants (τ_{act}) of currents from experiments as above, and from ClC-7$_{\Delta CT}$ + Ostm1-ClC-7$_{CT-R762L}$ in which a ClC-7 C terminus carrying the fast mutation R762L in CBS2 is fused to the Ostm1 β-subunit. *D*, activation time constants of WT ClC-7 compared with split transporters in which the truncation point after helix R is varied. ClC-7$_{1-623}$ corresponds to ClC-7$_{\Delta CT}$. Constructs were always co-expressed with ClC-7$_{CT}$ and with Ostm1. *Thick lines* indicate arithmetic mean, and *thin lines* indicate $\pm$ S.E. Significance levels (one-way analysis of variance): ***, $p < 0.001$.

amino acids, although the mechanism by which this changes gating remains unclear.

DISCUSSION

A fascinating aspect of the CLC family is that its members transport ions in modes traditionally thought to be radically different; they function either as ion channels or as strictly coupled ion exchangers. However, remnants of an ion exchange activity can be found in CLC Cl⁻ channels because the gating of ClC-0 may be associated with H⁺ transport (49). Further, the strong voltage dependence of Cl⁻/H⁺ exchange activity of vesicular CLCs resembles the gating of ion channels, as recently demonstrated for plasma membrane-expressed ClC-7 (14). The intrinsically almost linear anion/proton exchange activity of this transporter is very slowly turned on by depolarization in a process that strongly resembles gating of ion channels.

We now asked whether the gating of ClC-7/Ostm1 resembles the ClC-0 protopore gate, which affects one pore at a time, or its common gate, which closes both pores of the double-barreled channel simultaneously. We argued that mutations accelerating ClC-7 gating might impose their faster gating kinetics on associated WT subunits in heterodimers if the gating process involves both subunits. We devised experiments in which one of the subunits of the dimer was rendered transport-deficient by another mutation to better isolate the effect on the currents of the other subunit. Such transport-deficient mutants indeed partially imposed their gating kinetics on the other, transporting subunit, rendering their activation and deactivation faster or slower, depending on the particular combination. These results resemble previous work in which dominant ClC-1 mutants partially imposed their shifted voltage dependence (as observed in homomeric channels) on the gating of heteromers through an effect on common gating (18, 41). We conclude that voltage-dependent activation of ClC-7/Ostm1 prominently involves common gating of both subunits. A minor contribution of protopore gating, however, cannot be excluded.

Many accelerating mutations cluster in cytoplasmic CBS domains and the cytoplasmic surface of the ClC-7 transmembrane segment (14), suggesting that interactions between these parts of the protein influence gating. We have also explored another possible mechanism by which mutations in the C terminus could affect gating, *i.e.* through a direct "pull" of the C terminus on the last intramembrane helix R. This speculation is attractive because the N-terminal part of helix R participates in coordinating a Cl⁻ ion in a binding site in the permeation pathway as revealed by crystal structures of prokaryotic CLCs (9, 23). Consistent with this idea, Förster resonance energy transfer (FRET) experiments using ClC-0 and ClC-1 to whose C termini GFP variants had been fused indicated large movements of those domains during gating (27, 28). Although initial experiments in which we varied the length of the R helix-CBS1 linker seemed to support this hypothesis, our subsequent split transporter experiments clearly indicated that this is not the case.

These split transporter experiments indicated that the ClC-7 C terminus binds efficiently to the ClC-7 backbone even without being anchored nearby at the plasma membrane (as in the Ostm1-ClC-7$_{CT}$ fusion protein). The crystal structure of the

CBS domain-containing algal CLC (10) suggests that this binding prominently involves CBS2, a domain in which several osteopetrosis-causing mutations were found (14, 36, 43, 47). The similar gating kinetics of currents obtained from WT and ClC-7$_{\Delta CT}$ co-expressed with either Ostm1-ClC-7$_{CT}$ or the detached C terminus ClC-7$_{CT}$ suggest that the C terminus does not fully dissociate from the ClC-7 backbone during gating because its dilution in the cytoplasm is expected to severely slow down its reassociation. This should then be accompanied by a severe deceleration of either activation or deactivation, depending on whether the binding of the C terminus "closes" or "opens" the transporter, respectively. Interestingly, when we inserted fast mutations into CBS2, we observed functional split transporters only when the mutated C terminus was attached to Ostm1 (Fig. 5*C*), but not when it was supplied as a soluble protein. Hence these mutations may destabilize the binding of the C terminus to the transporter backbone with reasonably efficient binding occurring only when the local concentration of the C terminus is drastically increased by tethering it to Ostm1.

Split channel (respectively, transporter) approaches have been used previously with ClC-0 (50), ClC-1 (48, 51–54), and ClC-5 (55). These studies agreed in that the function of CLC proteins that were truncated after CBS1 could be rescued by co-expressing the missing fragment containing CBS2. This complementation can be easily explained by the tight CBS1-CBS2 binding that was revealed by crystal structures of CLC CBS domains (10, 56). Indeed, CBS domains also form internal dimers in other CBS domain-containing proteins (57). A complementation similar to the one described here, *i.e.* the functional rescue of a CLC truncated directly after the R helix by the complete soluble C terminus, had been tried previously with the skeletal muscle Cl⁻ channel ClC-1 (48, 54). However, both studies agreed that the co-expression of both fragments failed to yield functional channels. Hence the binding affinity of the backbone to the C-terminal tail seems to be stronger in the case of ClC-7.

Common gating requires a coordinate conformational change of both subunits of the dimer that ultimately leads to an occlusion of the permeation pathway. This necessitates both changes at the interface between both subunits and of residues in the pore region. CLC monomers contact each other not only at their broad membrane-embedded interface (9, 10), but also between the CBS domains of either subunit (10, 58). Consistent with these considerations, FRET detected large movements of CBS domains during common gating of ClC-0 (27), ¹⁹F NMR indicated substrate-driven changes in the position of a tyrosine at the membrane-embedded dimer interface of EcClC-1 (59), and mutations in the gating glutamate in the pore abolish both common and protopore gating of *e.g.* ClC-2 (21). However, our picture of common gating remains appallingly incomplete. In particular, the way in which mutations in CBS domains affect this gating process remains enigmatic.

Many mutations, not just those found in patients with osteopetrosis, accelerate ClC-7 gating, whereas we have not yet obtained ClC-7 mutants that gate more slowly than WT.[4] Evolution may have maximized the time constant of ClC-7 gating

---

that is several orders of magnitude slower than with ClC-3 to ClC-6. Together with the fact that many disease-causing mutations accelerate ClC-7 gating (14), these observations suggest that slow gating of ClC-7 may be important for its biological function. If accelerated gating by itself were pathogenic, the acceleration of common gating in WT/fast heteromers might contribute to the dominant inheritance pattern of some osteopetrosis-causing *CLCN7* mutations. However, some accelerating mutations may also decrease protein stability, as shown previously (36) for the R762Q mutant we have studied here. Indeed, this particular accelerating mutation was found in a patient with recessive osteopetrosis (36).

In summary, the gating of ClC-7/Ostm1 bears parallels to the common, slow gate of the *Torpedo* Cl⁻ channel ClC-0 that affects both pores of the dimeric channel simultaneously. It depends on the presence of the CBS domain-containing C terminus that interacts with the transmembrane backbone and modulates gating kinetics even in the absence of a covalent link. Our work extends the role of common gating from CLC Cl⁻ channels to Cl⁻/H⁺ exchangers.

REFERENCES

1. Jentsch, T. J., Steinmeyer, K., and Schwarz, G. (1990) Primary structure of *Torpedo marmorata* chloride channel isolated by expression cloning in *Xenopus* oocytes. *Nature* **348,** 510–514
2. Jentsch, T. J. (2008) CLC chloride channels and transporters: From genes to protein structure, pathology and physiology. *Crit. Rev. Biochem. Mol. Biol.* **43,** 3–36
3. Stauber, T., Weinert, S., and Jentsch, T. J. (2012) Cell biology and physiology of CLC chloride channels and transporters. *Compr. Physiol.* **2,** 1701–1744
4. Miller, C. (2006) ClC chloride channels viewed through a transporter lens. *Nature* **440,** 484–489
5. Accardi, A., and Miller, C. (2004) Secondary active transport mediated by a prokaryotic homologue of ClC Cl⁻ channels. *Nature* **427,** 803–807
6. Ludewig, U., Pusch, M., and Jentsch, T. J. (1996) Two physically distinct pores in the dimeric ClC-0 chloride channel. *Nature* **383,** 340–343
7. Middleton, R. E., Pheasant, D. J., and Miller, C. (1996) Homodimeric architecture of a ClC-type chloride ion channel. *Nature* **383,** 337–340
8. Weinreich, F., and Jentsch, T. J. (2001) Pores formed by single subunits in mixed dimers of different CLC chloride channels. *J. Biol. Chem.* **276,** 2347–2353
9. Dutzler, R., Campbell, E. B., Cadene, M., Chait, B. T., and MacKinnon, R. (2002) X-ray structure of a ClC chloride channel at 3.0 Å reveals the molecular basis of anion selectivity. *Nature* **415,** 287–294
10. Feng, L., Campbell, E. B., Hsiung, Y., and MacKinnon, R. (2010) Structure of a eukaryotic CLC transporter defines an intermediate state in the transport cycle. *Science* **330,** 635–641
11. Estévez, R., Boettger, T., Stein, V., Birkenhäger, R., Otto, E., Hildebrandt, F., and Jentsch, T. J. (2001) Barttin is a Cl⁻-channel β-subunit crucial for renal Cl⁻-reabsorption and inner ear K⁺-secretion. *Nature* **414,** 558–561
12. Lange, P. F., Wartosch, L., Jentsch, T. J., and Fuhrmann, J. C. (2006) ClC-7 requires Ostm1 as a β-subunit to support bone resorption and lysosomal function. *Nature* **440,** 220–223
13. Jeworutzki, E., López-Hernández, T., Capdevila-Nortes, X., Sirisi, S., Bengtsson, L., Montolio, M., Zifarelli, G., Arnedo, T., Müller, C. S., Schulte, U., Nunes, V., Martínez, A., Jentsch, T. J., Gasull, X., Pusch, M., and Estévez, R. (2012) GlialCAM, a protein defective in a leukodystrophy, serves as a ClC-2 Cl⁻ channel auxiliary subunit. *Neuron* **73,** 951–961
14. Leisle, L., Ludwig, C. F., Wagner, F. A., Jentsch, T. J., and Stauber, T. (2011)

15. ClC-7 is a slowly voltage-gated 2Cl⁻/1H⁺-exchanger and requires Ostm1 for transport activity. *EMBO J.* **30,** 2140–2152
15. Miller, C., and White, M. M. (1984) Dimeric structure of single chloride channels from *Torpedo* electroplax. *Proc. Natl. Acad. Sci. U.S.A.* **81,** 2772–2775
16. Bauer, C. K., Steinmeyer, K., Schwarz, J. R., and Jentsch, T. J. (1991) Completely functional double-barreled chloride channel expressed from a single *Torpedo* cDNA. *Proc. Natl. Acad. Sci. U.S.A.* **88,** 11052–11056
17. Ludewig, U., Pusch, M., and Jentsch, T. J. (1997) Independent gating of single pores in CLC-0 chloride channels. *Biophys. J.* **73,** 789–797
18. Saviane, C., Conti, F., and Pusch, M. (1999) The muscle chloride channel ClC-1 has a double-barreled appearance that is differentially affected in dominant and recessive myotonia. *J. Gen. Physiol.* **113,** 457–468
19. Chen, M. F., and Chen, T. Y. (2001) Different fast-gate regulation by external Cl⁻ and H⁺ of the muscle-type ClC chloride channels. *J. Gen. Physiol.* **118,** 23–32
20. de Santiago, J. A., Nehrke, K., and Arreola, J. (2005) Quantitative analysis of the voltage-dependent gating of mouse parotid ClC-2 chloride channel. *J. Gen. Physiol.* **126,** 591–603
21. Yusef, Y. R., Zúñiga, L., Catalán, M., Niemeyer, M. I., Cid, L. P., and Sepúlveda, F. V. (2006) Removal of gating in voltage-dependent ClC-2 chloride channel by point mutations affecting the pore and C-terminus CBS-2 domain. *J. Physiol.* **572,** 173–181
22. Bennetts, B., Yu, Y., Chen, T. Y., and Parker, M. W. (2012) Intracellular β-nicotinamide adenine dinucleotide inhibits the skeletal muscle ClC-1 chloride channel. *J. Biol. Chem.* **287,** 25808–25820
23. Dutzler, R., Campbell, E. B., and MacKinnon, R. (2003) Gating the selectivity filter in ClC chloride channels. *Science* **300,** 108–112
24. Traverso, S., Zifarelli, G., Aiello, R., and Pusch, M. (2006) Proton sensing of ClC-0 mutant E166D. *J. Gen. Physiol.* **127,** 51–65
25. Cederholm, J. M., Rychkov, G. Y., Bagley, C. J., and Bretag, A. H. (2010) Inter-subunit communication and fast gate integrity are important for common gating in hClC-1. *Int. J. Biochem. Cell Biol.* **42,** 1182–1188
26. Fong, P., Rehfeldt, A., and Jentsch, T. J. (1998) Determinants of slow gating in ClC-0, the voltage-gated chloride channel of *Torpedo marmorata*. *Am. J. Physiol.* **274,** C966–C973
27. Bykova, E. A., Zhang, X. D., Chen, T. Y., and Zheng, J. (2006) Large movement in the C terminus of ClC-0 chloride channel during slow gating. *Nat. Struct. Mol. Biol.* **13,** 1115–1119
28. Ma, L., Rychkov, G. Y., Bykova, E. A., Zheng, J., and Bretag, A. H. (2011) Movement of hClC-1 C-termini during common gating and limits on their cytoplasmic location. *Biochem. J.* **436,** 415–428
29. Lin, Y. W., Lin, C. W., and Chen, T. Y. (1999) Elimination of the slow gating of ClC-0 chloride channel by a point mutation. *J. Gen. Physiol.* **114,** 1–12
30. Stauber, T., and Jentsch, T. J. (2013) Chloride in vesicular trafficking and function. *Annu. Rev. Physiol.* **75,** 453–477
31. Friedrich, T., Breiderhoff, T., and Jentsch, T. J. (1999) Mutational analysis demonstrates that ClC-4 and ClC-5 directly mediate plasma membrane currents. *J. Biol. Chem.* **274,** 896–902
32. Li, X., Shimada, K., Showalter, L. A., and Weinman, S. A. (2000) Biophysical properties of ClC-3 differentiate it from swelling-activated chloride channels in Chinese hamster ovary-K1 cells. *J. Biol. Chem.* **275,** 35994–35998
33. Steinmeyer, K., Schwappach, B., Bens, M., Vandewalle, A., and Jentsch, T. J. (1995) Cloning and functional expression of rat CLC-5, a chloride channel related to kidney disease. *J. Biol. Chem.* **270,** 31172–31177
34. Neagoe, I., Stauber, T., Fidzinski, P., Bergsdorf, E. Y., and Jentsch, T. J. (2010) The late endosomal ClC-6 mediates proton/chloride countertransport in heterologous plasma membrane expression. *J. Biol. Chem.* **285,** 21689–21697
35. Stauber, T., and Jentsch, T. J. (2010) Sorting motifs of the endosomal/lysosomal CLC chloride transporters. *J. Biol. Chem.* **285,** 34537–34548
36. Kornak, U., Kasper, D., Bösl, M. R., Kaiser, E., Schweizer, M., Schulz, A., Friedrich, W., Delling, G., and Jentsch, T. J. (2001) Loss of the ClC-7 chloride channel leads to osteopetrosis in mice and man. *Cell* **104,** 205–215
37. Kasper, D., Planells-Cases, R., Fuhrmann, J. C., Scheel, O., Zeitz, O., Ru-

ether, K., Schmitt, A., Poët, M., Steinfeld, R., Schweizer, M., Kornak, U., and Jentsch, T. J. (2005) Loss of the chloride channel ClC-7 leads to lysosomal storage disease and neurodegeneration. *EMBO J.* **24,** 1079 –1091

38. Chalhoub, N., Benachenhou, N., Rajapurohitam, V., Pata, M., Ferron, M., Frattini, A., Villa, A., and Vacher, J. (2003) Grey-lethal mutation induces severe malignant autosomal recessive osteopetrosis in mouse and human. *Nat. Med.* **9,** 399 – 406

39. Weinert, S., Jabs, S., Supanchart, C., Schweizer, M., Gimber, N., Richter, M., Rademann, J., Stauber, T., Kornak, U., and Jentsch, T. J. (2010) Lysosomal pathology and osteopetrosis upon loss of H^+-driven lysosomal Cl^- accumulation. *Science* **328,** 1401–1403

40. Lorenz, C., Pusch, M., and Jentsch, T. J. (1996) Heteromultimeric CLC chloride channels with novel properties. *Proc. Natl. Acad. Sci. U.S.A.* **93,** 13362–13366

41. Pusch, M., Steinmeyer, K., Koch, M. C., and Jentsch, T. J. (1995) Mutations in dominant human myotonia congenita drastically alter the voltage dependence of the ClC-1 chloride channel. *Neuron* **15,** 1455–1463

42. Zdebik, A. A., Zifarelli, G., Bergsdorf, E.-Y., Soliani, P., Scheel, O., Jentsch, T. J., and Pusch, M. (2008) Determinants of anion-proton coupling in mammalian endosomal CLC proteins. *J. Biol. Chem.* **283,** 4219 – 4227

43. Cleiren, E., Bénichou, O., Van Hul, E., Gram, J., Bollerslev, J., Singer, F. R., Beaverson, K., Aledo, A., Whyte, M. P., Yoneyama, T., deVernejoul, M. C., and Van Hul, W. (2001) Albers-Schönberg disease (autosomal dominant osteopetrosis, type II) results from mutations in the *ClCN7* chloride channel gene. *Hum. Mol. Genet.* **10,** 2861–2867

44. Accardi, A., Walden, M., Nguitragool, W., Jayaram, H., Williams, C., and Miller, C. (2005) Separate ion pathways in a Cl^-/H^+ exchanger. *J. Gen. Physiol.* **126,** 563–570

45. Bergsdorf, E. Y., Zdebik, A. A., and Jentsch, T. J. (2009) Residues important for nitrate/proton coupling in plant and mammalian CLC transporters. *J. Biol. Chem.* **284,** 11184 –11193

46. Zifarelli, G., and Pusch, M. (2009) Conversion of the 2 Cl^-/1 H^+ antiporter ClC-5 in a NO_3^-/H^+ antiporter by a single point mutation. *EMBO J.* **28,** 175–182

47. Frattini, A., Pangrazio, A., Susani, L., Sobacchi, C., Mirolo, M., Abinun, M., Andolina, M., Flanagan, A., Horwitz, E. M., Mihci, E., Notarangelo, L. D., Ramenghi, U., Teti, A., Van Hove, J., Vujic, D., Young, T., Albertini, A., Orchard, P. J., Vezzoni, P., and Villa, A. (2003) Chloride channel *ClCN7* mutations are responsible for severe recessive, dominant, and intermediate osteopetrosis. *J. Bone Miner Res.* **18,** 1740 –1747

48. Schmidt-Rose, T., and Jentsch, T. J. (1997) Reconstitution of functional voltage-gated chloride channels from complementary fragments of CLC-1. *J. Biol. Chem.* **272,** 20515–20521

49. Lísal, J., and Maduke, M. (2008) The ClC-0 chloride channel is a 'broken' Cl^-/H^+ antiporter. *Nat. Struct. Mol. Biol.* **15,** 805– 810

50. Maduke, M., Williams, C., and Miller, C. (1998) Formation of CLC-0 chloride channels from separated transmembrane and cytoplasmic domains. *Biochemistry* **37,** 1315–1321

51. Estévez, R., Pusch, M., Ferrer-Costa, C., Orozco, M., and Jentsch, T. J. (2004) Functional and structural conservation of CBS domains from CLC chloride channels. *J. Physiol.* **557,** 363–378

52. Wu, W., Rychkov, G. Y., Hughes, B. P., and Bretag, A. H. (2006) Functional complementation of truncated human skeletal-muscle chloride channel (hClC-1) using carboxyl tail fragments. *Biochem. J.* **395,** 89 –97

53. Ma, L., Rychkov, G. Y., Hughes, B. P., and Bretag, A. H. (2008) Analysis of carboxyl tail function in the skeletal muscle Cl^- channel hClC-1. *Biochem. J.* **413,** 61– 69

54. Hebeisen, S., Biela, A., Giese, B., Müller-Newen, G., Hidalgo, P., and Fahlke, C. (2004) The role of the carboxyl terminus in ClC chloride channel function. *J. Biol. Chem.* **279,** 13140 –13147

55. Mo, L., Xiong, W., Qian, T., Sun, H., and Wills, N. K. (2004) Coexpression of complementary fragments of ClC-5 and restoration of chloride channel function in a Dent's disease mutation. *Am. J. Physiol. Cell Physiol.* **286,** C79 –C89

56. Meyer, S., and Dutzler, R. (2006) Crystal structure of the cytoplasmic domain of the chloride channel ClC-0. *Structure* **14,** 299 –307

57. Ignoul, S., and Eggermont, J. (2005) CBS domains: structure, function, and pathology in human proteins. *Am. J. Physiol. Cell Physiol.* **289,** C1369-C1378

58. Markovic, S., and Dutzler, R. (2007) The structure of the cytoplasmic domain of the chloride channel ClC-Ka reveals a conserved interaction interface. *Structure* **15,** 715–725

59. Elvington, S. M., Liu, C. W., and Maduke, M. C. (2009) Substrate-driven conformational changes in ClC-ec1 observed by fluorine NMR. *EMBO J.* **28,** 3090 –3102